Stressed solid-phase epitaxial growth of (011) Si

N.G. Rudawski[a] and K.S. Jones
Department of Materials Science and Engineering, University of Florida, Gainesville, Florida 32611-6400

R. Gwilliam
Nodus Accelerator Laboratory, Advanced Technology Institute, Surrey Ion Beam Centre, Guildford, Surrey GU2 7XH, United Kingdom

(Received 16 July 2008; accepted 17 September 2008)

The solid-phase epitaxial growth kinetics of amorphized (011) Si with application of in-plane $[2\bar{1}1]$ uniaxial stress to magnitude of 0.9 ± 0.1 GPa were studied. Tensile stresses did not appreciably change the growth velocity compared with the stress-free case, whereas compression tended to retard the growth velocity to approximately one-half the stress-free value. The results are explained using a prior generalized atomistic model of stressed solid-solid phase transformations. In conjunction with prior observations of stressed solid-phase epitaxial growth of (001) Si, it is advanced that the activation volume tensor associated with ledge migration may be substrate orientation-dependent.

Stressed solid-phase epitaxial growth (SPEG) of Si amorphized via ion-implantation has become a topic of greater technological interest during the past several years due to the importance of SPEG in doping Si-based devices and the increasingly prevalent nature of stresses typically present during fabrication.[1,2] The stressed-SPEG process has been studied in (001) Si under a variety of different stress states, including pure hydrostatic stress,[3–7] uniaxial stress applied parallel to the growth direction,[8] and in-plane uniaxial stress applied perpendicular to the growth direction.[9–11] Currently, (001) Si is used for both p- and n-type transistor in the vast majority of Si-based devices. However, there is growing interest in the use of hybrid orientation technology wafers that contain both (001)- and (011)-oriented sections.[12–14] In particular, the use of (011) Si is attractive for p-type transistors due to the inherently faster hole mobility and larger piezoresistive coefficients compared with (001) Si.[15,16]

SPEG of (011) Si has been studied far less compared with (001) Si. In fact, little else is known beyond the observations by Csepregi et al. who revealed (011)-oriented SPEG to be much slower than (001)-oriented SPEG.[17] Thus, the goal of this work is to study the stressed-SPEG process of (011) Si and determine how (011)-oriented stressed-SPEG differs from (001)-oriented stressed-SPEG.

In this study, a polished 50-μm-thick (011) Si wafer was Si^+ implanted at 50, 100, and 200 keV to doses of 1×10^{15}, 1×10^{15}, and 3×10^{15} cm^{-2} and subsequently As^+ implanted at 300 keV to a dose of 1.8×10^{15} cm^{-2}. The wafer was subsequently cleaved along the in-plane $[2\bar{1}1]$ direction into $\sim 0.2 \times 1.8$ cm^2 strips (with 1 and 2 axes taken to be $[2\bar{1}1]$ and $[11\bar{1}]$ crystal directions). Uniaxial stress up to magnitude of 0.9 GPa along $[2\bar{1}1]$ (σ_{11}) was applied using the method presented elsewhere.[18] By convention, positive (negative) values of σ_{11} are tensile (compressive). The error in all $\sigma_{11} \neq 0$ is estimated to be ± 0.1 GPa. Stress-free, tensilely stressed, and compressively stressed strips were annealed simultaneously at 525 ± 1 °C in N_2 ambient up to 1.5 h with no detectable stress relaxation occurring for any stressed samples. The addition of As (from As^+ implantation) was necessary to enhance growth kinetics[19] such that appreciable growth could be observed before the onset of appreciable stress relaxation. The SPEG process was examined using on-axis cross-sectional transmission electron microscopy (XTEM). Approximately 40 XTEM specimens ~10-μm long were prepared via site-specific focused ion beam (FIB) milling within a distance of ±4.2 mm from the strip centers to minimize the presence of any thermal gradient. Due to the very small specimen length to strip length ratio, it is reasonably assumed no intraspecimen stress gradients existed.

Figures 1(a) and 1(e) display XTEM micrographs of the as-implanted structure, indicating an initial amorphous (α) Si layer 327 ± 3 nm thick. Annealing for 1.5 h with $\sigma_{11} = 0$ resulted in 128 ± 3 nm of growth (epitaxial crystallization of α-Si) with a planar resulting α/crystalline (growth) interface as shown in Fig. 1(f). The error in the as-implanted α-Si layer thickness and subsequent growth measurements is given as the root-mean-squared roughness of the α/crystalline interface in each case. End of range (EOR) damage near the initial α/crystalline interface resulting from ion-implantation

[a]Address all correspondence to this author.
e-mail: ngr@ufl.edu
DOI: 10.1557/JMR.2009.0056

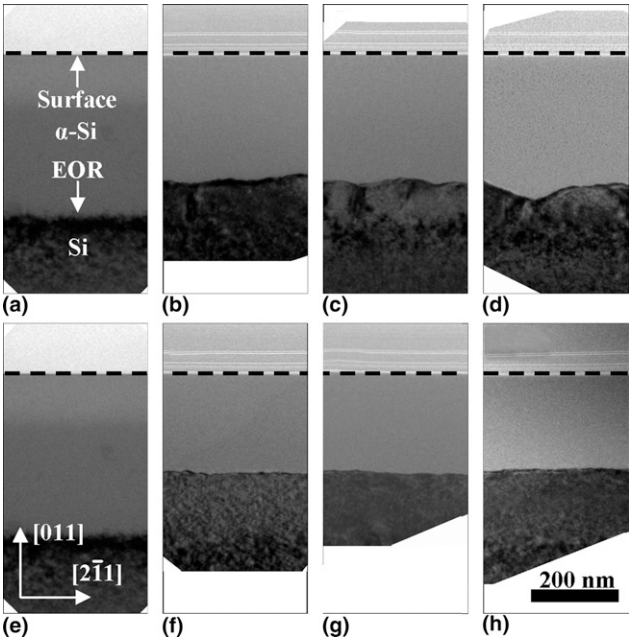

FIG. 1. (a, e) XTEM images of the as-implanted structure. XTEM images of specimens annealed for 1.5 h at 525 °C with applied in-plane [2$\bar{1}$1] uniaxial stress of (b) −0.25, (c) −0.5, (d) −0.9, (f) 0, (g) 0.5, and (h) 0.9 GPa.

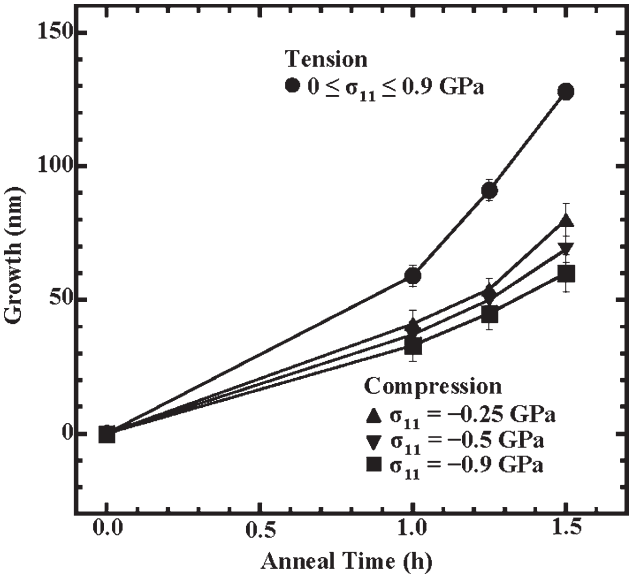

FIG. 2. Plot of (011)-oriented growth (epitaxial crystallization of amorphous Si) versus anneal time behavior at 525 °C for different applied in-plane [2$\bar{1}$1] uniaxial stresses (σ_{11}).

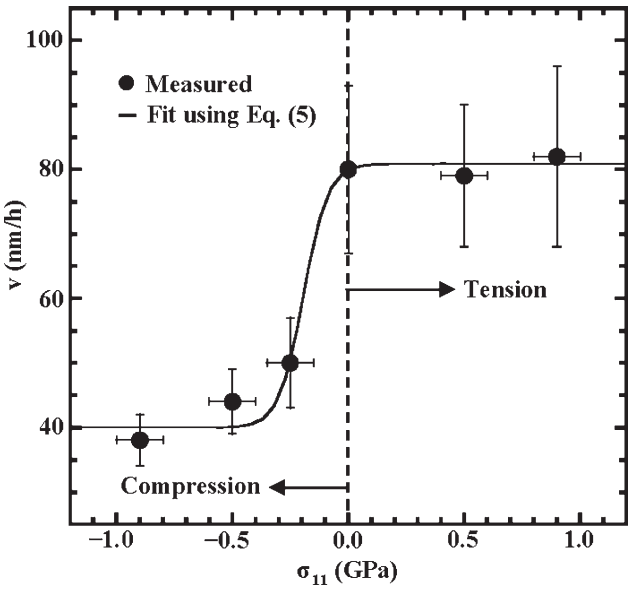

FIG. 3. Plot of the time-averaged (011)-oriented growth velocity (v) at 525 °C versus applied in-plane [2$\bar{1}$1] uniaxial stress (σ_{11}).

was present in all samples.[20] In the case of annealing for 1.5 h with $\sigma_{11} = -0.25$, -0.5, and -0.9 GPa (compression), shown in Figs. 1(b)–1(d), 100 ± 6, 69 ± 5, and 60 ± 7 nm of growth occurred, which is less than the $\sigma_{11} = 0$ case. The growth interface was observed to roughen with $\sigma_{11} < 0$, similarly to reports of kinetically driven instability for stressed SPEG of (001) Si.[10,21,22] In contrast, annealing with $\sigma_{11} = 0.5$ and 0.9 GPa (tension), shown in Figs. 1(g) and 1(h), produced nominally the same amount of growth as the $\sigma_{11} = 0$ case. These observations are qualitatively consistent with recent studies of stressed SPEG of (001) Si.[10,11]

Growth as a function of anneal time was measured for different σ_{11} as shown in Fig. 2. In tension, the growth versus time behavior was nominally the same for all σ_{11} in this range, and thus only the $\sigma_{11} = 0$ set of data is reported for clarity. The growth kinetics for compression were greatly retarded compared with the $0 \leq \sigma_{11}$ cases. For all σ_{11}, the growth kinetics appear to vary with anneal time, which is presumably due to the variable As concentration from the As^+-implantation step.[19]

Figure 3 displays a plot of the time-averaged growth interface velocity, v, versus σ_{11} estimated from the data of Fig. 2 using standard least-squares regression analysis techniques. The growth velocity was nearly constant with $0 \leq \sigma_{11}$ with $v = 80 \pm 12$ nm/h. However, v rapidly decreased to near 38 ± 4 nm/h with $\sigma_{11} \ll 0$, close to one-half the value observed with $0 \leq \sigma_{11}$. These observations are very similar to those observed in stressed SPEG of intrinsic (001) Si.[10,11]

It is important to note the presence of As in this work, which is known to enhance SPEG in the absence of stress and may therefore be a complicating factor.[19] However, As-enhanced SPEG was necessary to induce appreciable growth before stress relaxation because growth of intrinsic (011) Si is much slower than intrinsic (001) Si.[17] Barvosa-Carter and Aziz[23] suggested that dopant and stress influences on growth kinetics were independent and separable, but recent work by Rudawski et al.[24] suggested possible dopant-stress synergy for certain stress states in the case of (001)-oriented growth.

In the present work on (011) Si, it is unclear if impurity and stress effects are independent or synergistic and thus, for purposes of clarity, a time-averaged approach has been taken to modeling the growth kinetics. It should be noted that the error in all v calculations (Fig. 3) accounts for the apparent As-influenced temporal variability in the growth versus time behavior (Fig. 2) via standard least-squares regression error analysis.

SPEG is the result of crystal island nucleation in the growth interface with subsequent in-plane migration of island ledges.[25,26] In terms of macroscopic growth kinetics, the two processes must be modeled as sequential because growth is the result of a solid-solid phase transformation.[10] For (001) Si, v as a function of σ_{11} applied along the [110] crystal direction [1 axis in the case of (001)-oriented growth] was shown to be given by

$$v = \frac{\Delta x}{\tau_n(0) + 2^{-3/2}\tau_{m,11}(0)\exp\left(\frac{-\Delta V_{11}^{m,11}\sigma_{11}}{kT}\right)} + \frac{\Delta x}{\tau_n(0) + 2^{-3/2}\tau_{m,11}(0)} \quad , \tag{1}$$

where $\Delta x = 0.14$ nm is the monolayer spacing, $\tau_{m,11}(0)$ is the stress-free timescale for ledge migration along 1, $\tau_n(0)$ is the stress-free timescale for crystal island nucleation, $\Delta V_{11}^{m,11}$ is the activation volume for ledge migration along 1 in the 1 direction (longitudinal activation volume along 1) and kT has the usual meaning.[10,11]

For (011) Si, it is reasonable to expect nucleation kinetics to be independent of in-plane stress because the activation volume tensor associated with nucleation possess no in-plane components.[10,11] The ledge migration tensor, $\tau_{m,ij}^{-1}$, for the α-Si/(011) Si interface (without stress) for the chosen coordinate frame of reference is of the form

$$\tau_{m,ij}^{-1} = \begin{pmatrix} \tau_{m,11}^{-1} & \tau_{m,12}^{-1} \\ \tau_{m,21}^{-1} & \tau_{m,22}^{-1} \end{pmatrix} \quad . \tag{2}$$

In contrast, $\tau_{m,ij}^{-1}$ is isotropic for the α-Si/(001) Si interface without stress.[11] The application of σ_{kl} alters $\tau_{m,ij}^{-1}$ as given by

$$\tau_{m,ij} = \tau_{m,ij}(0)^{-1}\exp\left(\frac{\Delta V_{kl}^{m,ij}\sigma_{kl}}{kT}\right) \quad , \tag{3}$$

where $\tau_{m,ij}(0)^{-1}$ is the stress-free value of $\tau_{m,ij}^{-1}$ and $\Delta V_{kl}^{m,ij}$ is the ledge migration activation volume tensor for $\tau_{m,ij}^{-1}$.[11] Using a prior generalized model of stressed solid-solid phase transformations,[10] and neglecting the shear components of $\tau_{m,ij}^{-1}$, v as a function of σ_{11} for (011) Si can be shown to be given by

$$v = \frac{\Delta x}{\tau_n(0) + \frac{\tau_{m,11}(0)}{2\sqrt{3}}\exp\left(\frac{-\Delta V_{11}^{m,11}\sigma_{11}}{kT}\right)} + \frac{\Delta x}{\tau_n(0) + \frac{1}{4}\sqrt{\frac{2}{3}}\tau_{m,22}(0)\exp\left(\frac{-\Delta V_{11}^{m,22}\sigma_{11}}{kT}\right)} \quad , \tag{4}$$

where $\Delta x = 0.19$ nm, and the nonexponential coefficients of the two migration timescales are reflective of the crystallographic nature of the chosen coordinate frame of reference.[11]

As per Eq. (4) and the data from Fig. 3, it appears that migration in one direction is being influenced by σ_{11}, whereas migration in the other direction is not. In work of stressed SPEG of (001) Si, it was advanced that the longitudinal activation volume along 1 ($\Delta V_{11}^{m,11}$) associated with ledge migration should be much greater than the transverse activation volume ($\Delta V_{11}^{m,22}$). Presumably, this also applies to the (011) Si system in the chosen coordinate frame of reference and thus $\tau_{m,22} \sim \tau_{m,22}(0)$ because $|\Delta V_{11}^{m,22}| \ll |\Delta V_{11}^{m,11}|$ and Eq. (4) can be simplified further to

$$v = \frac{\Delta x}{\tau_n(0) + \frac{\tau_{m,11}(0)}{2\sqrt{3}}\exp\left(\frac{-\Delta V_{11}^{m,11}\sigma_{11}}{kT}\right)} + \frac{\Delta x}{\tau_n(0) + \frac{1}{4}\sqrt{\frac{2}{3}}\tau_{m,22}(0)} \quad . \tag{5}$$

Equation (5) was fit to the data presented in Fig. 3, producing $\tau_n(0) = 4.7 \pm 0.5 \times 10^{-3}$ h, $\tau_{m,11}(0) = 4.1 \pm 0.4 \times 10^{-4}$ h, $\tau_{m,22}(0) = 5.6 \pm 0.5 \times 10^{-4}$ h, and $\Delta V_{11}^{m,11} = (10.6 \pm 1.0)\ \Omega$, where Ω is the atomic volume of Si. The value of $\Delta V_{11}^{m,11}$ for (011) Si reported here is of similar magnitude compared with $\Delta V_{11}^{m,11} = (12.0 \pm 1.0)\ \Omega$ reported for (001) Si,[10,11] which suggests that coordinated atomic rearrangement[27,28] is involved for ledge migration during (011) SPEG similarly to the (001) case.[10,11] Also, the observation that $\tau_n(0) > \tau_{m,11}(0)$ and$\tau_{m,22}(0)$ and $\tau_{m,11}(0) \neq \tau_{m,22}(0)$ suggests that (011)-oriented SPEG is nucleation limited [similar to (001)-oriented SPEG] and that $\tau_{m,ij}^{-1}(0)$ is anisotropic for the α-Si/(011) Si interface (as predicted). Equation (5) can also readily predict the growth interface roughening with σ_{11}, similarly to the case of stressed SPEG of (001) Si as presented elsewhere.[10]

It should be noted that the coordinate frame used for this study [as dictated by the cleaving behavior of (011) Si] is not the simplest one possible for (011) Si. Rather,

the simplest coordinate frame would use $[01\bar{1}]$ and [100] in-plane crystal directions as 1 and 2 axes. Thus, the migration activation volume tensor for this orientation, $\Delta V_{kl}^{m,ij0}$, would have longitudinal activation volumes $\Delta V_{11}^{m,110}$ and $\Delta V_{22}^{m,220}$ and negligible transverse and shear activation volumes. By transforming this coordinate frame to the frame using $[2\bar{1}1]$ and $[11\bar{1}]$ as the 1 and 2 axes (used in this work), it can be shown that

$$\Delta V_{11}^{m,11} \sim \frac{1}{9}\left(\Delta V_{11}^{m,110} + 4\Delta V_{22}^{m,220}\right) \quad , \qquad (6)$$

and

$$\Delta V_{11}^{m,22} \sim \frac{2}{9}\left(\Delta V_{11}^{m,110} + \Delta V_{22}^{m,220}\right) \quad . \qquad (7)$$

As was stated earlier, $\Delta V_{11}^{m,11} = (10.6 \pm 1.0)\ \Omega$ and $|\Delta V_{11}^{m,22}| \ll |\Delta V_{11}^{m,11}|$ thus implying $\Delta V_{11}^{m,110} = -\Delta V_{22}^{m,220}$ and $-3\Delta V_{11}^{m,11} \sim \Delta V_{11}^{m,110}$ as per Eqs. (6) and (7). Thus, $\Delta V_{11}^{m,110}$ is predicted to be negative, and this provides an interesting set of predictions regarding stress-influenced growth kinetics. For example, if uniaxial stress was applied along $[01\bar{1}]$ during (011)-oriented SPEG, it is therefore predicted that compression should not cause any SPEG enhancement, whereas tension should cause SPEG retardation. This is the opposite trend observed for uniaxial stress applied along $[2\bar{1}1]$ during growth. Also, because the magnitude of $\Delta V_{11}^{m,110}$ is greater than $\Delta V_{11}^{m,11}$, the predicted decrease in v for uniaxial tension along $[01\bar{1}]$ should occur at a much smaller magnitude of stress compared with uniaxial compression along $[2\bar{1}1]$. The growth interface would also be predicted to roughen with tension rather than compression. Experiments are underway to test these predictions.

In the case of the α-Si/(001) Si interface, $\Delta V_{11}^{m,110} = \Delta V_{22}^{m,220} = (12 \pm 1)\ \Omega$ with 1 and 2 axes taken as <110>-type in-plane crystal directions.[10,11] Using an argument similar to that presented for the α-Si/(011) Si interface, it can be shown that v should always be unchanged (retarded) with in-plane tension (compression) with application of uniaxial stress along any in-plane crystal direction for (001)-oriented growth. This is in stark contrast to the predictions of stressed SPEG in (011) Si, where it is predicted that growth kinetics would be unchanged (retarded) with in-plane compression (tension) for application of uniaxial stress along $[01\bar{1}]$. Thus, as per the prior results of (001)-oriented SPEG and the presented (011)-oriented results, $\Delta V_{kl}^{m,ij}$ may be growth orientation-dependent. This advancement is quite reasonable, particularly in light of the significant differences in the atomic arrangements between each orientation.

In summary, the solid-phase epitaxial growth kinetics of (011) Si under applied stress were examined. Application of tensile in-plane uniaxial stress along $[2\bar{1}1]$ did not greatly change the growth kinetics compared with the stress-free case, whereas compression caused retardation of the growth velocity to approximate one-half the stress-free value. These observations were similar to those of recent work in stressed solid-phase epitaxial growth of (001) Si. As per the utilized coordinate frame and the calculated activation volume for ledge migration, it was also predicted that the growth velocity versus in-plane uniaxial stress behavior may be different depending on the crystallographic direction of the applied stress. In a larger context, the results suggest that the activation volume tensor associated with ledge migration may be substrate orientation-dependent.

ACKNOWLEDGMENTS

We acknowledge the Semiconductor Research Corporation for funding this research and the Major Analytical Instrumentation Center at the University of Florida for use of the TEM and FIB facilities.

REFERENCES

1. G.L. Olsen and J.A. Roth: Kinetics of solid phase crystallization of amorphous silicon. *Mater. Sci. Rep.* **3,** 1 (1988).
2. S.M. Hu: Stress-related problems in silicon technology. *J. Appl. Phys.* **70**(6), R53 (1991).
3. E. Nygren, M.J. Aziz, and D. Turnbull: Effect of pressure on the solid phase epitaxial regrowth rate of Si. *Appl. Phys. Lett.* **47**(3), 232 (1985).
4. G-Q. Lu, E. Nygren, M.J. Aziz, D. Turnbull, and C.W. White: Interferometric measurement of the pressure-enhanced crystallization rate of amorphous Si. *Appl. Phys. Lett.* **54,** 2583 (1989).
5. G-Q. Lu, E. Nygren, and M.J. Aziz: Pressure-enhanced crystallization kinetics of amorphous Si and Ge: Implications for point-defect mechanisms. *J. Appl. Phys.* **70**(10), 5323 (1991).
6. T.K. Chaki: Hydrostatic pressure-enhanced solid-phase epitaxy. *Philos. Mag. Lett.* **63**(6), 303 (1991).
7. T.K. Chaki: Solid-phase epitaxy—Effects of irradiation, dopant, and pressure. *Phys. Status Solidi A* **142**(1), 153 (1994).
8. W. Barvosa-Carter: Stress effects on kinetics and interfacial roughening during solid phase epitaxy. Ph.D. Thesis, 1997.
9. M.J. Aziz, P.C. Sabin, and G-Q. Lu: The activation strain tensor Nonhydrostatic effects on crystal-growth kinetics. *Phys. Rev. B: Condens. Matter* **44**(18), 9812 (1991).
10. N.G. Rudawski, K.S. Jones, and R. Gwilliam: Kinetics and morphological instabilities of stressed solid-solid phase transformations. *Phys. Rev. Lett.* **100**(16), 165501 (2008).
11. N.G. Rudawski, K.S. Jones, and R. Gwilliam: Stressed solid-phase epitaxial growth of ion-implanted amorphous silicon. *Mater. Sci. Eng., R* **61,** 40 (2008).
12. K.L. Saenger, J.P. de Souza, K.E. Fogel, J.A. Ott, A. Reznicek, C.Y. Sung, D.K. Sadana, and H. Yin: Amorphization/templated recrystallization method for changing the orientation of single-crystal silicon: An alternative approach to hybrid orientation substrates. *Appl. Phys. Lett.* **87**, 221911 (2005).
13. K.L. Saenger, J.P. de Souza, K.E. Fogel, J.A. Ott, C.Y. Sung, D.K. Sadana, and H. Yin: A study of trench-edge defect formation in (001) and (011) silicon recrystallized by solid phase epitaxy. *J. Appl. Phys.* **101,** 024908 (2006).
14. M. Yang, V.W.C. Chan, K.K. Chan, L. Shi, D.M. Fried, J.H. Stathis, A.I. Chou, E. Gusev, J.A. Ott, L.E. Burns,

M.V. Fischetti, and M. Ieong: Hybrid orientation technology (HOT): Opportunities and challenges. *IEEE Trans. Electron Devices* **53**(5), 965 (2005).
15. T. Sato, Y. Takeishi, and H. Hara: Effects of crystallographic orientation on mobility, surface state density, and noise in p-type inversion layers on oxidized silicon surfaces. *Jpn. J. Appl. Phys.* **8** (5), 588 (1969).
16. D. Colman, R.T. Bate, and J.P. Mize: Mobility anisotropy and piezoresistance in silicon p-type inversion layers. *J. Appl. Phys.* **39**(4), 1923 (1968).
17. L. Csepregi, E.F. Kennedy, and T.W. Sigmon: Substrate-orientation dependence of the epitaxial regrowth rate of Si-implanted amorphous Si. *J. Appl. Phys.* **49**(7), 3906 (1978).
18. N.G. Rudawski, K.S. Jones, and R. Gwilliam: Solid phase epitaxy in uniaxially stressed (001) Si. *Appl. Phys. Lett.* **91,** 172103 (2007).
19. B.C. Johnson and J.C. McCallum: Dopant-enhanced solid-phase epitaxy in buried amorphous silicon layers. *Phys. Rev. B* **76**(4), 045206 (2007).
20. K.S. Jones, S. Prussin, and E.R. Weber: A systematic analysis of defects in ion-implanted silicon. *Appl. Phys. A* **45**(1), 1 (1988).
21. W. Barvosa-Carter, M.J. Aziz, L.J. Gray, and T. Kaplan: Kinetically driven growth instability in stressed solids. *Phys. Rev. Lett.* **81**(7), 1445 (1998).
22. W. Barvosa-Carter, M.J. Aziz, A-V. Phan, T. Kaplan, and L.J. Gray: Interfacial roughening during solid phase epitaxy: Interaction of dopant, stress, and anisotropy effects. *J. Appl. Phys.* **96**(10), 5462 (2004).
23. W. Barvosa-Carter and M.J. Aziz: Time-resolved measurements of stress effects on solid-phase epitaxy of intrinsic and doped Si. *Appl. Phys. Lett.* **79,** 356 (2001).
24. N.G. Rudawski, K.S. Jones, and R. Gwilliam: Dopant-stress synergy in Si solid-phase epitaxy. *Appl. Phys. Lett.* **92,** 232110 (2008).
25. F. Spaepen: A structural model for the interface between amorphous and crystalline Si or Ge. *Acta Metall.* **26,** 1167 (1978).
26. J.S. Williams, R.G. Elliman, W.L. Brown, and T.E. Seidel: Dominant influence of beam-induced interface rearrangement on solid-phase epitaxial crystallization of amorphous silicon. *Phys. Rev. Lett.* **55**(14), 1482 (1985).
27. R.J. Asaro and S. Suresha: Mechanistic models for the activation volume and rate sensitivity in metals with nanocrystalline grains and nano-scale twins. *Acta Mater.* **53,** 3369 (2005).
28. Y.M. Wang, A.V. Hamza, and E. Ma: Temperature-dependent strain rate sensitivity and activation volume of nanocrystalline Ni. *Acta Mater.* **54,** 2715 (2006).